# Comparative Analysis of Impedance Based and Travelling Wave Based Fault Location Techniques

Olutoye S. and Ezechukwu O. A.
Department of Electrical Engineering, Nnamdi Azikiwe University, Awka, Anambra State.

**ABSTRACT**

One of the major problems in power system is the occurrence of disturbances that affect the quality of electricity supply. Fault location detection is therefore the key to reliable operation of power equipments and satisfactory service delivery with minimum interruption. This need has given rise to fault location techniques so that the effects of fault can be mitigated with appropriate corrective measures. This paper, thus, presents two algorithmic approaches towards fault location detection with and without using transmission line parameters. A comparison between these techniques, that is the impedance-based method and travelling wave-based method was done to ascertain their level of efficacy in estimating the distance of various faults at different locations on the transmission line. The modelling and simulations were done using Simulink and the algorithms of both methods were written using MATLAB codes. Lower the value of percentage error, better the accuracy of algorithm.

## 1. Introduction

Accurate estimation of fault location is very useful when lines are long and run through inaccessible areas where patrolling is difficult and time-consuming. Several methods of locating transmission line faults are now available. The primitive method of fault location was to visually inspect the line (T.W. Stringfield, D. J. Marihart and R. F. Stevens, 1957). The procedure involved patrolling the line by foot or automobile and inspecting the line with or without the aid of binoculars. Sectionalizing the line and energizing it in parts has been used to reduce the length of the line that must be inspected. These procedures are slow, inaccurate and expensive, and are unsafe during adverse weather conditions.

Thus, the techniques of fault location are travelling-wave based methods, intelligence based method, impedance measurement based methods and high frequency components of currents and voltages generated by faults based methods (Kurt, 2007). This paper, however, compares the accuracy of the results obtained from impedance measurement based method and travelling wave based method.

## 2. Impedance-Based Fault Location Methods

The one-line diagram of a faulted transmission line is shown in Figure 1. The transmission line connects source S and source R at each terminal equipped with IED. $V_S$ and $V_R$ are the measured terminal voltages. $I_S$ and $I_R$ are the measured currents from both terminals. $Z_L$ represents the impedance of the entire line. When a fault occurs somewhere on the line with total length L, the distance from terminal S to the fault location is defined as m. Consequently, the distance from terminal R to the fault location is defined as $L - m$. The voltage and total fault current at the fault location is named as $V_F$ and $I_F$.
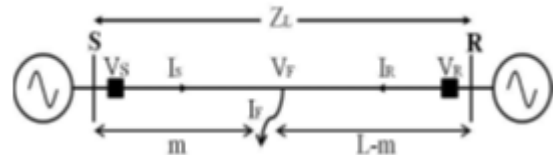


**Figure 1. One-line Diagram of a Faulted Transmission Line.**

### 2.1. One-End Positive Sequence Reactance Method

One-end positive-sequence-reactance method is based on the symmetrical component model of the transmission line. It is assumed that the transmission line is ideally transposed and the phase wires have equal spacing. This results in the equal mutual coupling between phases. The principle of positive-sequence-reactance method can be explained by using fault analysis for a single-line-to-ground fault. Figure 2 gives the symmetrical component circuit model of an A-phase-to-ground fault on the line at a distance m from the sending end.
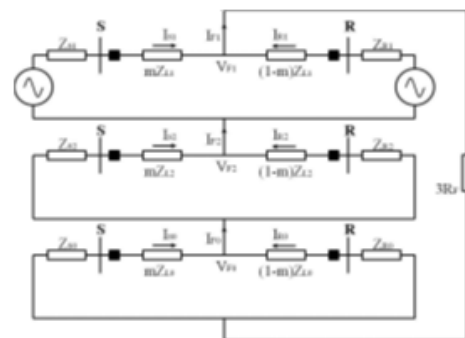


**Figure 2. Symmetrical Component Circuits for A-G Fault.**

Tele:
E-mail address: sampraise1981@gmail.com

The voltage drop from the sending terminal to the fault location can be expressed as;

$$V_{S1} = mZ_{L1}I_{S1} + V_{F1} \qquad (1)$$
$$V_{S2} = mZ_{L2}I_{S2} + V_{F2} \qquad (2)$$
$$V_{S0} = mZ_{L0}I_{S0} + V_{F0} \qquad (3)$$

The summation of the three equations results in;

$$V_{Sa} = mZ_{L1}I_{S1} + mZ_{L2}I_{S2} + mZ_{L0}I_{S0} + V_{Fa} \qquad (4)$$

Since $Z_{L1}, Z_{L2}$ is assumed to be equal and $I_{S1} = I_{S2} = I_{S0} = \frac{1}{3}I_F$ for phase to ground fault, $V_{Fa} = R_F I_F$. Equation (4) can be rewritten as:

$$V_{Sa} = mZ_{L1}[I_{Sa} + kI_{S0}] + R_F I_F \qquad (5)$$

Where factor $k = \frac{Z_{L0}-Z_{L1}}{Z_{L1}}$

The voltage and current $V_S$ and $I_S$ is defined as;

$$V_S = V_{Sa}$$
$$(6)$$
$$I_S = I_{Sa} + kI_{S0} \qquad (7)$$

So equation (5) can be expressed as

$$V_S = mZ_{L1}I_S + R_F I_F \qquad (8)$$

The selection of $V_S$ and $I_S$ depends on the fault type, as given in Table1.

**Table1. Selection of measurements for different fault types.**

| Fault Type | $V_S$ | $I_S$ |
|---|---|---|
| A-G | $V_a$ | $I_a + k \cdot I_0$ |
| B-G | $V_b$ | $I_b + k \cdot I_0$ |
| C-G | $V_c$ | $I_c + k \cdot I_0$ |
| A-B or A-B-G | $V_{ab}$ | $I_{ab}$ |
| B-C or B-C-G | $V_{bc}$ | $I_{bc}$ |
| C-A or C-A-G | $V_{ca}$ | $I_{ca}$ |
| A-B-C or A-B-C-G | Any of $V_{ab}, V_{bc}, V_{ca}$ | Any of $I_{ab}, I_{bc}, I_{ca}$ |

The apparent reactance measured at terminal S can be obtained by dividing equation (8) by $I_S$.

$$\frac{V_S}{I_S} = mZ_{L1} + R_F \frac{I_F}{I_S} \qquad (9)$$

To compensate the effect of fault resistance, only the imaginary part of equation (9) is computed.

$$Im\left(\frac{V_S}{I_S}\right) = m \cdot Im(Z_{L1}) + Im\left(R_F \frac{I_F}{I_S}\right) \qquad (10)$$

If complex number $I_f$ and $I_S$ have the same phase angle or $R_F$ is negligible, we will obtain,

$$m = \frac{Im\left(\frac{V_S}{I_S}\right)}{X_{L1}} \qquad (11)$$

## 2.2. One-End Takagi Method

The Takagi method introduced superposed current $I_{sup}$ to eliminate the effect of power flow on fault location accuracy. Therefore, this method assumes constant current load model and requires both pre-fault and post-fault data.

$$I_{sup} = I_s - I_{pre} \qquad (12)$$

Where $I_{pre}$ is the pre-fault current. If we multiply equation (8) by the conjugate of $I_{sup}$ and extracting the imaginary part, we will obtain,

$$Im(V_s \cdot I_{sup}^*) = m \cdot Im(Z_{L1} \cdot I_s \cdot I_{sup}^*) + Im(R_F \cdot I_s \cdot I_{sup}^*) \qquad (13)$$

If complex number $I_F$ and $I_{sup}$ have the same angle or $R_F$ is negligible, we will obtain,

$$m = \frac{Im(V_s \cdot I_{sup}^*)}{Im(Z_{L1} \cdot I_s \cdot I_{sup}^*)} \qquad (14)$$

## 2.3. Two-End Negative-Sequence Method

Two-end negative-sequence method uses data at both terminals of the transmission line. By using negative-sequence component, the effects of pre-fault power flow and fault resistance are eliminated. Unlike one-end methods, negative-sequence method requires source impedance to perform fault location estimation. Figure 3 shows the negative sequence circuit of a faulted transmission line.
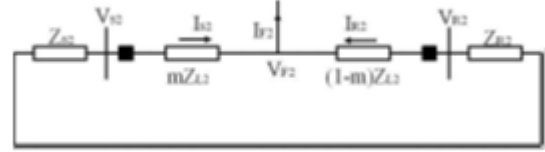


**Figure 3. Negative-sequence circuit of a faulted transmission line.**

At source S,

$$V_{F2} = -I_{S2} \cdot (Z_{S2} + m \cdot Z_{L2}) \qquad (15)$$

At source R,

$$V_{F2} = I_{R2} \cdot [Z_{S2} + (1 - m) \cdot Z_{L2}] \qquad (16)$$

By equalizing equation (15) and (16), we can obtain,

$$I_{F2} = I_{R2} \cdot \frac{Z_{S2}+m \cdot Z_{L2}}{Z_{S2}+(1-m) \cdot Z_{L2}} \qquad (17)$$

Taking the magnitude of both sides and simplifying the equation, a quadratic equation can be obtained to calculate the fault location estimation.

## 2.4. Two-End Three Phase Impedance Matrix Method

A fault location algorithm based on the three-phase line impedance matrix method is being developed and implemented in this paper. This method is not only applicable to transmission lines, but also distribution feeders. Using Figure1 as the one-line diagram, the voltage at two terminals of the line can be expressed as;

At source S,

$$V_{sabc} = m \cdot Z_{Labc} \cdot I_{sabc} + V_{fabc} \qquad (18)$$

At source R,

$$V_{rabc} = (1 - m) \cdot Z_{Labc} \cdot I_{rabc} + V_{fabc} \qquad (19)$$

Where;

$$V_{sabc} = \begin{bmatrix} V_{sa} \\ V_{sb} \\ V_{sc} \end{bmatrix}$$ is the three phase terminal voltage measured at source S,

$$I_{sabc} = \begin{bmatrix} I_{sa} \\ I_{sb} \\ I_{sc} \end{bmatrix}$$ is the three phase terminal current measured at source S,

$$V_{rabc} = \begin{bmatrix} V_{ra} \\ V_{rb} \\ V_{rc} \end{bmatrix}$$ is the three phase terminal voltage measured at source R,

$$I_{rabc} = \begin{bmatrix} I_{ra} \\ I_{rb} \\ I_{rc} \end{bmatrix}$$ is the three phase terminal current measured at source R,

$$Z_{Labc} = \begin{bmatrix} Z_{aa} & Z_{ab} & Z_{ac} \\ Z_{ba} & Z_{bb} & Z_{bc} \\ Z_{ca} & Z_{cb} & Z_{cc} \end{bmatrix}$$ is the three phase line impedance matrix

$$V_{fabc} = \begin{bmatrix} V_{fa} \\ V_{fb} \\ V_{fc} \end{bmatrix}$$ is the three phase voltage at the fault location.

Subtracting equation (18) from (19), we can obtain,

$$V_{sabc} - V_{rabc} + Z_{Labc} \cdot I_{rabc} = m \cdot Z_{Labc}(I_{sabc} + I_{rabc})$$

(20)

$V_{sabc}, I_{sabc}, V_{rabc}, I_{rabc}$ are measured quantities and is known if line configuration data is available. Let

$$Y = V_{sabc} - V_{rabc} + Z_{Labc} \cdot I_{rabc}$$

(21)

$$D = Z_{Labc}(I_{sabc} + I_{rabc})$$

(22)

Equation (20) becomes equation (23), which contains three complex equations and six real equations.

$$Y = m \cdot D \qquad (23)$$

Least-square estimation can be applied to determine the only unknown parameter m. Suppose fault occurs at some point which is m distance away from terminal A. $V_f$ is fault voltage, the fault voltage is given

$$(V_f)_i = (V_A)_i - mZ_i * (I_A)_i \qquad (24)$$

$$(V_f)_i = (V_B)_i - (1 - m)Z_i * (I_B)_i$$

(25)

Where, i =0,1,2 for zero, positive and negative sequence

$Z_s$= source impedance

m=fault distance from terminal A on transmission line

$V_A$, $V_B$= Three phase fault voltages at terminal A and B respectively

$I_A$, $I_B$= Three phase fault currents at terminal A and B respectively

Z= line impedance which is equal to R + jX

Equating equation (24) and (25)

$$(V_A)_i - (V_B)_i + Z_i(I_B)_i = m * Z_i(I_{Ai} + I_{Bi})$$

(26)

Data from Bus A and Bus B are not synchronized. So, synchronization angle, $\delta$ is added to equation (26) to make the two terminals synchronized. So, terminal voltages at terminal A and B becomes

$$(V_A)_i = (V_A)_i \angle \alpha_i + \delta \qquad (27)$$

$$(V_B)_i = (V_B)_i \angle \beta_i \qquad (28)$$

Similarly, equation for current is

$$(I_A)_i = (I_A)_i \angle \gamma_i + \delta \qquad (29)$$

$$(I_B)_i = (I_B)_i \angle \theta_i$$

(30)

Where,

α, β, γ, θ = measured angles

Equation (26) can be written as

$$(V_A)_i e^{j\delta} - (V_B)_i + Z_i(I_B)_i = m * Z_i * (I_{Ai}e^{j\delta} + I_{Bi})$$

(31)

Synchronization angle, δ can be expressed as cos(δ) + jsin(δ). Equation (31) is expressed into real and imaginary components as:

$$Re(V_A)_i \sin\delta + Im(V_A)_i \cos\delta - Im(V_B)_i + (C_4)_i = m((C_1)_i \sin\delta + (C_2)_i \cos\delta + (C_4)_i) \qquad (32)$$

$$Re(V_A)_i \cos\delta + Im(V_A)_i \sin\delta - Re(V_B)_i + C_{3i} = m((C_1)_i \cos\delta - (C_2)_i \sin\delta + (C_3)_i) \qquad (33)$$

Where,

$$(C_1)_i = R_i * Re(I_A)_i - X_i * Im(I_A)_i \qquad (34)$$

$$(C_2)_i = R_i * Im(I_A)_i - X_i * Re(I_A)_i \qquad (35)$$

$$(C_3)_i = R_i * Re(I_B)_i - X_i * Im(I_B)_i \qquad (36)$$

$$(C_4)_i = R_i * Im(I_B)_i - X_i * Re(I_B)_i \qquad (37)$$

To find δ, equation (32) is divided by (33) and removing a number of terms, following equations are developed:

$$a_i * \sin\delta + b_i \cos\delta + C_i = 0 \qquad (38)$$

Where,

$$a_i = (C_3)_i Re(V_A)_i - (C_4)_i Im(V_A)_i - (C_1)_i Re(V_B)_i - (C_2)_i Im(V_B)_i + (C_1)_i(C_3)_i + (C_2)_i(C_4)_i \qquad (39)$$

$$b_i = (C_4)_i Re(V_A)_i - (C_3)_i Im(V_A)_i - (C_2)_i Re(V_B)_i + (C_1)_i Im(V_B)_i + (C_2)_i(C_3)_i + (C_1)_i(C_4)_i \qquad (40)$$

$$c_i = -(C_2)_i Re(V_A)_i - (C_1)_i Im(V_A)_i - (C_4)_i Re(V_B)_i + (C_3)_i Im(V_B)_i \qquad (41)$$

The synchronization angle, $\delta$ is determined by an iterative Newton - Raphson Method. The equations for the iteration are

$$\delta_{k+1} = \delta_k - \frac{F(\delta_k)}{\dot{F}(\delta_k)}$$

(42)

$$F(\delta_k) = b_i * \cos\delta_k + a_i * \sin\delta_k + C_i \qquad (43)$$

$$\dot{F}(\delta_k) = b_i * \cos\delta_k - b_i * \sin\delta_k \qquad (44)$$

This method requires initial guess for δ. The iteration is terminated when the difference between $\delta_{k+1}$ and δ is smaller than the specified tolerance. Once the synchronization angle is determined, fault location m is calculated from equations (32) and (33).

If equation (32) is used, fault distance is:

$$m = \frac{Re(V_A)_i \sin\delta + Im(V_A)_i \cos\delta - Im(V_B)_i + (C_4)_i}{(C_1)_i \sin\delta + (C_2)_i \cos\delta + (C_4)_i)} \qquad (45)$$

If equation (33) is used, fault distance is:

$$m = \frac{Re(V_A)_i \cos\delta - Im(V_A)_i \sin\delta - Re(V_B)_i + (C_3)_i}{(C_1)_i \cos\delta - (C_2)_i \sin\delta + (C_3)_i)} \qquad (46)$$

## 3. Travelling Wave Method

Traveling wave recorders (TWR) are assumed to be placed at the end of the line. From the recorded fault voltages and currents, transient time taken by surge to travel from the fault point to TWR is known. If the propagation velocity of the wave is known, distance to fault from any station can be calculated. The propagation velocity of the wave depends on the value of line parameter such as (inductance (L) and capacitance(C)). The fault location is greatly dependent on propagation speed of the traveling waves.

The transient wave might have other frequency components that propagate along the line. To find the dominant frequency, two methods are used widely (Emmanouil Styvaktakis, Mathias H.J. Bollen, Irene Y.H. Gu, (1999). The first approach is spectrum estimation and the second approach is wavelet transform. Wavelet transform is used to extract the dominant frequency from the transient wave. Daubechies wavelet is used to detect and locate the disturbance event (S. Santoso, E. Powers, W. Grady, and P. Hoffmann, 1996).

Daubechies wavelet has many filter coefficients like Daub4, Daub6, Daub8, and Daub10.
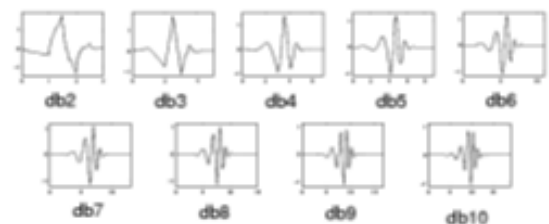


**Figure 3. Nine Members of Daubechies Family.**

(S. Santoso, E. J. Powers and W. M. Grady, 1994) presented that Daub4 and Daub6 wavelets are better for those power system disturbances, which are short and fast. Daub8 and Daub10 wavelet are suitable for those

disturbances, which are slow transient. In this paper, Daub6 wavelet was used. In three-phase transmission lines, traveling waves are mutually coupled, so there is no single travelling wave velocity. The phase domain signals are decomposed into their modal components by using modal transformation. In this method, all transmission line are assumed to be fully transposed and therefore the well-known Clarke's constant and real transformation matrix is used:

$$T = \begin{bmatrix} 1 & 1 & 1 \\ 2 & -1 & -1 \\ 0 & \sqrt{3} & -\sqrt{3} \end{bmatrix} \qquad (47)$$

Where $T$ is the transformation matrix. The phase signals are transformed into their modal components by using transformation matrix as follows:

$$S_{mode} = TS_{phase} \qquad (48)$$

Where $S_{mode}$ is the modal vectors and $S_{phase}$ is the phase signals vectors (voltage or current). Equation (48) transformed the recorded phase signals into their modal components. There are two modes: ground mode and aerial mode. The ground mode is also called mode1 and the aerial mode is also called mode 2. The ground mode is suitable for grounded faults. Therefore, this mode is not suitable for all types of faults. The aerial mode is suitable for both grounded and ungrounded faults.

In Single-ended algorithm, there is no need to synchronize with the remote end of transmission lines. Fault currents or voltages are taken from one end of the line and are transformed into their modal components using (48). Fault distance is calculated with the difference in the reflection time of two consecutive traveling waves from the fault point to that end.

## 4.1. Ungrounded Fault

The ungrounded fault involves no significant reflection from the remote end bus. So fault distance is calculated by taking the product of wave velocity and half of the time delay between two consecutive peaks in the wavelet transform coefficient. Fault distance is calculated using the equation below:

$$x = \frac{vt_d}{2} \qquad (49)$$

Where $v$ is the wave velocity of the traveling waves, $t_d$ is the time difference of the first two peaks of aerial mode wavelet transform coefficient in scale 5.

## 4.2. Grounded Fault

In the grounded fault, reflection from the remote-end bus should be considered depending upon the location of the fault on the line. The reflected wave from the remote end bus may arrive after and before the reflected wave from the fault point. This can be verified using Lattice diagram.



**Figure 5(a). Remote End Fault**
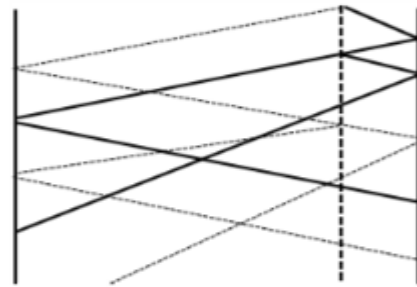


**Figure 5(b). Lattice Diagram of Remote-End Fault of Figure 5a.**

From the figure 5, at terminal A the first peak is the wave away from fault point. Second wave is the reflected wave from terminal B.



**Figure 6(a). Close End Fault.**
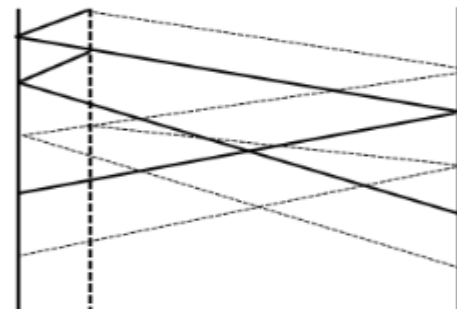


**Figure 6(b). Lattice Diagram of Close-In Fault of Figure 6a.**

If fault occurs at first half of length of the line, wave from the remote end bus arrive before the reflected wave from fault point. From the above close-in and remote-end fault, it is clear that reflected wave from the remote-end bus always arrive after the reflection from the fault point, if and only if, fault occurs at close half of length of the line. If fault occurs at remote-end of the line, $t_d$ in equation (49) is the difference of first two peaks in scale 5. The two peaks are wavelet transform coefficient of aerial mode. If the fault occurs within second half of the line, $t_d$ is replaced by $t_r$ as in equation (50).

$$t_r = 2\tau - t_x \qquad (50)$$

Where $\tau$ is the travel time for entire line length and $t_x$ is the time difference between the first two peaks of aerial mode wavelet transform coefficient in scale 5.

## 5. Description of the Simulation Model

The transmission line has been modelled using distributed parameters so that it accurately describes a long transmission line. A snapshot of the model used for obtaining the data sets is as shown in Figure 7.

In this Figure 7, Z1 and Z2 are the source impedances of the generators on either side. The three-phase V - I measurement block is used to measure the voltage and current samples at the terminal B. The transmission line (Line 1 and Line 2 together) are 100km long and three-phase fault block is used to inject various types of faults at varying locations along the transmission line with different fault resistances.
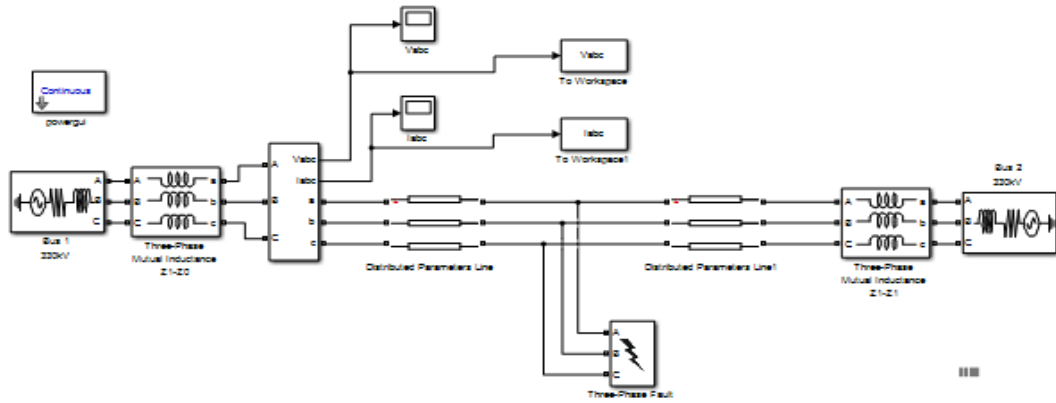
**Figure 7. Simulink Model of Faulted Three-Phase Transmission Line.**

## 6. Simulations and Results of Impedance Based Method
### 6.1 Simulations
The transmission line model measuring 100km from Bus 1 to Bus 2 was simulated under the applications of different fault types at varying location. All the fault types were initiated between 0.05s and 0.08s. The measured fault voltage and fault current values at Bus 2 were sampled and sent to MATLAB workspace from where the impedance based algorithm to compute the fault distance as presented in Table 2.

### 6.2 Results
Table 2 shows the fault location accuracy (i.e. percentage errors) in fault estimations for various fault types at various locations. In the tabulated results, it is glaring that the percentage error is above unity at 65km and 85km of single phase to ground fault. The same occurrence observed at 15km of double phase to ground fault as well as at 55km and 75km of balance three-phase fault. Al others tend to zeros, which demonstrate the level of efficacy of this algorithm.

**Table 2. Fault location estimations for four types of fault at different locations on the transmission line using impedance based method algorithm.**

| Fault Types | Actual Fault Location from Bus 2 (km) | Calculated Fault Distance (km) | Percentage Error |
|---|---|---|---|
| Single phase to ground fault (on phase A) | 15 | 14.06 | 0.94 |
| | 25 | 25.68 | 0.68 |
| | 35 | 35.87 | 0.87 |
| | 45 | 45.53 | 0.53 |
| | 55 | 55.92 | 0.92 |
| | 65 | 66.02 | 1.02 |
| | 75 | 75.82 | 0.82 |
| | 85 | 86.54 | 1.54 |
| Double phase to ground fault (on phase A & B) | 15 | 16.00 | 1.00 |
| | 25 | 25.55 | 0.55 |
| | 35 | 35.87 | 0.87 |
| | 45 | 45.67 | 0.67 |
| | 55 | 55.31 | 0.31 |
| | 65 | 65.91 | 0.91 |
| | 75 | 75.63 | 0.63 |
| | 85 | 86.01 | 1.01 |
| Double phase fault (on phase B & C) | 15 | 14.22 | 0.78 |
| | 25 | 25.89 | 0.89 |
| | 35 | 35.79 | 0.79 |
| | 45 | 45.71 | 0.71 |
| | 55 | 55.31 | 0.31 |
| | 65 | 65.42 | 0.42 |
| | 75 | 75.45 | 0.45 |
| | 85 | 85.64 | 0.64 |
| Three Phase fault (on phase A, B and C) | 15 | 14.24 | 0.76 |
| | 25 | 25.81 | 0.81 |
| | 35 | 35.67 | 0.67 |
| | 45 | 45.43 | 0.43 |
| | 55 | 56.03 | 1.03 |
| | 65 | 65.32 | 0.32 |
| | 75 | 76.12 | 1.12 |
| | 85 | 85.87 | 0.87 |

## 7. Simulations and Results of Travelling Wave Based Method

### 7.1 Simulations

The values of the current and voltage obtained during fault simulation at different locations in SIMULINK environment were sampled at the frequency of 100MHz. The results were sent and stored in MATLAB workspace. The fault currents were transformed into their modal components: ground mode and aerial mode. Ground mode is significant only in grounded faults whereas aerial mode is significant for all types of faults. The speed of the wave is nearly equal to the speed of the light. So, higher sampling frequency 100MHz was used for accuracy. Sampling frequency of 100MHz was considered to be high enough to capture the traveling waves. The aerial mode current sampled waveforms were given as input to MATLAB.

In MATLAB, the sampled waveforms were decomposed into detail and approximation coefficient wavelets using high pass filter and low pass filters respectively. The approximation coefficients of wavelet transform were the smooth versions of the original signals. The detail coefficients have the detailed occurrence of disturbances. Further, sampled waveforms were broken down in 5 scales (scale 1,2,3,4 & 5) using daubechies 6 filters. The aerial mode detail coefficients at scale 5 were used to detect and locate the disturbance events of all fault types made at different locations on the transmission line model

### 7.2 Results

Table 3 shows the results of performance accuracy of this method. The calculated percentage errors are indications that this algorithm is very efficient in estimating fault distance as all the error margins due to it are infinitesimal.

**Table 3. Fault calculations for various fault types at various locations on transmission lines using travelling wave based method algorithm.**

| Fault Types | Actual Fault Location from Bus 2 (km) | Calculated Fault Distance (km) | Percentage Error |
|---|---|---|---|
| Single phase to ground fault (on phase A) | 15 | 14.15 | 0.85 |
| | 25 | 25.21 | 0.21 |
| | 35 | 35.19 | 0.19 |
| | 45 | 45.17 | 0.17 |
| | 55 | 55.31 | 0.31 |
| | 65 | 65.22 | 0.22 |
| | 75 | 75.32 | 0.32 |
| | 85 | 85.40 | 0.40 |
| Double phase to ground fault (on phase A & B) | 15 | 15.21 | 0.21 |
| | 25 | 25.11 | 0.11 |
| | 35 | 35.33 | 0.33 |
| | 45 | 45.21 | 0.21 |
| | 55 | 55.09 | 0.09 |
| | 65 | 65.32 | 0.32 |
| | 75 | 75.30 | 0.30 |
| | 85 | 85.11 | 0.11 |
| Double phase fault (on phase B & C) | 15 | 14.76 | 0.24 |
| | 25 | 26.00 | 1.00 |
| | 35 | 35.19 | 0.19 |
| | 45 | 45.33 | 0.33 |
| | 55 | 55.12 | 0.12 |
| | 65 | 65.21 | 0.21 |
| | 75 | 75.14 | 0.14 |
| | 85 | 85.33 | 0.33 |
| Three Phase fault (on phase A, B & C) | 15 | 15.14 | 0.14 |
| | 25 | 25.30 | 0.30 |
| | 35 | 35.21 | 0.21 |
| | 45 | 45.18 | 0.18 |
| | 55 | 55.21 | 0.21 |
| | 65 | 65.11 | 0.11 |
| | 75 | 76.22 | 1.22 |
| | 85 | 85.23 | 0.23 |

## 8. Comparison of the Precision and Accuracy of Impedance Based Method and Traveling Wave Method

In this thesis, the precision and accuracy of the results obtained from both methods is measured by comparing the percentage errors of their calculated results. Fault distance estimations on the transmission line and percentage errors as calculated are presented in Table 4.

$$\% \; Error = \frac{Actual \; Length - Estimated \; Location}{Total \; Length \; of \; the \; Line} * 100$$

Table 4 shows the percentage errors in fault calculations for various types of fault in both methods. It can be evidently seen that travelling wave based method has a better accuracy as almost all its percentage errors for various estimated fault locations are infinitesimal compared the impedance based method. This is, however, with exception in two instances of double phase fault (on phase B and C) at 25km and three phase fault (on phase A, B and C) at 75km where the percentage errors of travelling wave method is slightly more than that of impedance based method by 0.11 and 0.1 respectively.

**Table 4. Percentage error in fault calculations using impedance based method and traveling wave method.**

| Fault Types | Actual Fault Location from Bus 2 (km) | Calculated Distance Impedance based method (km) | Calculated Distance Traveling wave method(km) | % Error (Impedance based method) | % Error (Traveling wave method) |
|---|---|---|---|---|---|
| Single phase to ground fault (on phase A) | 15 | 14.06 | 14.15 | 0.94 | 0.15 |
| | 25 | 25.68 | 25.21 | 0.68 | 0.21 |
| | 35 | 35.87 | 35.19 | 0.87 | 0.19 |
| | 45 | 45.53 | 45.17 | 0.53 | 0.17 |
| | 55 | 55.92 | 55.31 | 0.92 | 0.31 |
| | 65 | 66.02 | 65.22 | 1.02 | 0.22 |
| | 75 | 75.82 | 75.32 | 0.82 | 0.32 |
| | 85 | 86.54 | 85.40 | 1.54 | 0.40 |
| Double phase to ground fault (on phase A & B) | 15 | 16.00 | 15.21 | 1.00 | 0.21 |
| | 25 | 25.55 | 25.11 | 0.55 | 0.11 |
| | 35 | 35.87 | 35.33 | 0.87 | 0.33 |
| | 45 | 45.67 | 45.21 | 0.67 | 0.21 |
| | 55 | 55.31 | 55.09 | 0.31 | 0.09 |
| | 65 | 65.91 | 65.32 | 0.91 | 0.32 |
| | 75 | 75.63 | 75.30 | 0.63 | 0.30 |
| | 85 | 86.01 | 85.11 | 1.01 | 0.11 |
| Double phase fault (on phase B & C) | 15 | 14.22 | 14.76 | 0.78 | 0.24 |
| | 25 | 25.89 | 26.00 | 0.89 | 1.00 |
| | 35 | 35.79 | 35.19 | 0.79 | 0.19 |
| | 45 | 45.71 | 45.33 | 0.71 | 0.33 |
| | 55 | 55.31 | 55.12 | 0.31 | 0.12 |
| | 65 | 65.42 | 65.21 | 0.42 | 0.21 |
| | 75 | 75.45 | 75.14 | 0.45 | 0.14 |
| | 85 | 85.64 | 85.33 | 0.64 | 0.33 |
| Three Phase fault (on phase A, B & C) | 15 | 14.24 | 15.14 | 0.76 | 0.14 |
| | 25 | 25.81 | 25.30 | 0.81 | 0.30 |
| | 35 | 35.67 | 35.21 | 0.67 | 0.21 |
| | 45 | 45.43 | 45.18 | 0.43 | 0.18 |
| | 55 | 56.03 | 55.21 | 1.03 | 0.21 |
| | 65 | 65.32 | 65.11 | 0.32 | 0.11 |
| | 75 | 76.12 | 76.22 | 1.12 | 1.22 |
| | 85 | 85.87 | 85.23 | 0.87 | 0.23 |

**7. Conclusion**

Faults may lead to considerable economic losses in power systems. Thus, fault location needs be determined with high accuracy as soon as possible. This paper gives exhaustive view of fault location computations on transmission line using impedance-based method and travelling wave based method.

The results obtained from MATLAB analysis show that the applied algorithms (i.e. impedance based method and travelling wave based method) were successful in determining the locations of different types of fault on the transmission line model. From the tabulated results, almost all the percentage errors due to travelling wave method at various fault locations for different fault types approximately tend to zeros (0s) unlike that of impedance based method whose values approximately equal to ones (1s). Thus, algorithm of travelling wave method can improve the performance accuracy of impedance based method.

**References**

Emmanouil Styvaktakis, Mathias H. J. Bollen, Irene Y.H., Gu (1999)."A Fault Location Technique Using High Frequency Fault Clearing Transients".

M. Kurt, (2007). "Fault Location on Three Terminal Over head Lines with using Two Terminal Synchronized Voltage and Current Phasors", International Symposium: Modern Electric Power System.

S. Santoso, E. J. Powers and W. M. Grady, (1994). "Electric power quality disturbance detection using wavelet transform analysis', Proceedings of the IEEE-SP International Symposium on Time-Frequency and Time-Scale Analysis.

S. Santoso, E. Powers, W. Grady, and P. Hoffmann, (1996). "Power Quality Assessment via Wavelet Transform Analysis", IEEE Transactions on Power Delivery, Vol.11.

T. W. Stringfield, D. J. Marihart and R. F. Stevens,(1957). "Fault Location Methods for Overhead Lines", Transactions of the AIEE, Part III, Power Apparatus and Systems, Vol. 76.